

Kinetics of the Hydrogenation of CO over a Single Crystal Nickel Catalyst

D. W. GOODMAN, R. D. KELLEY, T. E. MADEY, AND J. T. YATES, JR.

Surface Science Division, National Bureau of Standards, Washington, D.C. 20234

Received April 20, 1979; revised August 29, 1979

A specially designed ultrahigh vacuum system has been used to examine the effect of surface chemical composition on the kinetics of the catalytic methanation reaction over a single crystal Ni(100) catalyst. The surface is characterized using Auger Electron Spectroscopy (AES) in an ultrahigh vacuum chamber, and reaction kinetics are determined following an *in vacuo* transfer of the sample to a catalytic reactor contiguous to the AES chamber. The kinetics of CO hydrogenation on a clean Ni(100) surface at 450–800 K are compared with kinetic data reported for high-area supported nickel catalysts. Excellent agreement is observed between specific rates, activation energy, and product distribution measured for the supported catalysts and the single crystal Ni(100). The dependence of the specific rate on total pressure (1–1500 Torr) and on H₂ and CO partial pressures as well as the product distribution are also reported. These data are consistent with a mechanism in which an active surface carbon species is the dominant route to product.

I. INTRODUCTION

Considerable data have been accumulated regarding the nature of the interaction of molecules with low surface area metal surfaces. Modern ultrahigh vacuum techniques coupled with surface sensitive spectroscopies allow such experiments to be carried out on initially well-characterized surfaces. Single crystals are especially well suited for molecule–surface studies permitting measurements to be undertaken with a reduction of variables regarding the nature of the surface, i.e., lattice conformation, surface cleanliness, surface defects, etc. Studies on the idealized surfaces of single crystals have particular chemical significance if a correspondence exists between the chemistry observed to take place on these ordered, low surface area materials and the chemistry which occurs on a typical high surface area process catalyst. Recently, ultrahigh vacuum methods have been applied to catalytic studies on initially clean, low surface area metal surfaces of Pt (1), Rh (2), Fe (3) and Ni (4, 5). Specific

reaction rates over low area (~1 cm²) catalyst samples often agree with specific reaction rates for high area samples (~100 m²/g). These data suggest that low area well-characterized samples can be used as models for working catalysts in studies of catalytic reaction mechanisms as well as in studies of the mechanism of catalytic deactivation and poisoning.

We are presently using a specially designed ultrahigh vacuum system to examine the effect of surface structure and surface chemical composition on the kinetics of the catalytic methanation reaction (3H₂ + CO → CH₄ + H₂O). The catalyst sample is a high-purity single crystal of nickel whose surface is cut to expose (100) planes. The surface is characterized using Auger Electron Spectroscopy (AES) in an ultrahigh vacuum chamber and reaction kinetics are determined following an *in vacuo* transfer of the sample to a catalytic reactor contiguous to the AES chamber. A preliminary account of this work has already appeared (5).

We report here specific reaction rates

(product molecules/substrate surface atom/sec) for the catalytic methanation reaction over Ni(100) as a function of pressure (1–1500 Torr), temperature (450–800 K), and H₂/CO ratio (1–1000). This work permits the most extensive comparison to date between catalytic processes over single crystals and high area catalysts. The specific rate for CH₄ production, the activation energy, and product distribution over Ni(100) are in excellent agreement with similar data for high area Ni catalysts. The results are extremely sensitive to trace levels of surface impurity (Fe, S), and much care was required to ensure that the data are characteristic of a clean Ni surface.

A fractional monolayer quantity of a carbide-like form of carbon is found to be always present on the active catalyst following reaction and is identified as a precursor to methane formation. The kinetics of formation and subsequent hydrogenation of this carbide-like carbon suggest that the "active carbon" route, as opposed to an oxygenated complex (6, 8), is the primary route to methane product.

An outline of this paper is as follows. We begin in Section II with a discussion of the ultrahigh vacuum catalytic reactor, and of the experimental procedures. The Results (Section III) begins with a discussion of the reaction rates on an initially clean Ni(100) catalyst and a comparison of these rates with high area Ni catalysts. Next the formation of an active surface carbon is described followed by the effects of total pressure on the reaction rate.

II. EXPERIMENTAL

The apparatus used for this study is shown in Fig. 1. It consists of two ultrahigh vacuum chambers, both bakeable and capable of 10⁻¹⁰ Torr pressures. The surface analysis and preparation chamber is an ion-pumped system with a double pass cylindrical mirror analyzer for Auger analyses. A quadrupole mass spectrometer is available for residual gas analysis. The single crystal Ni(100) catalyst is a disc 0.6 cm in diameter

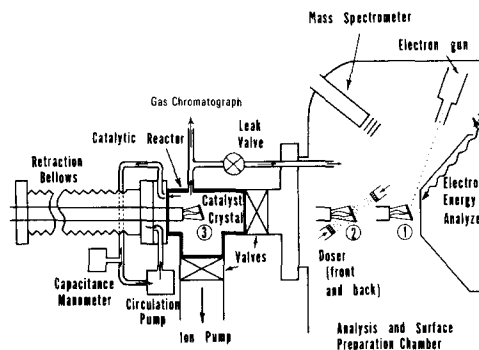


FIG. 1. Ultrahigh vacuum apparatus for studying single crystal catalysts before and after operation at high pressure in catalytic reactor. Position 1. Crystal is in position for Auger electron spectroscopy study of surface composition, or of ultraviolet photoemission spectrum of surface species. Position 2. Crystal is in position for deposition of a known coverage of poisons or promoters for a study of their influence on the rate of a catalytic reaction. Position 3. Crystal is in position for a study of catalytic reaction rate at elevated pressures, up to 2 atmospheres. Gas at high pressure may be circulated used pump; mass spectrometric/gas chromatographic analysis of the reactants/products is carried out by sampling the catalytic chamber.

and 0.1 cm thick, polished on both sides to expose (100) planes. It is spotwelded to two short high-purity Ni wires and is heated resistively so that the only heated metal in the reaction chamber is Ni. The sample is mounted on a retraction bellows and can be translated horizontally to various positions. In position (1), the surface chemical composition is determined using electron excited Auger spectroscopy; in position (2), the front and back of the crystal can be dosed with catalyst poisons or promoters using a molecular beam dosing array. Both positions (1) and (2) are in the UHV analysis and surface preparation chamber. In position (3), the catalyst is located in a stirred catalytic reactor. High-purity reactant gases, after passing through glass wool-filled traps at liquid nitrogen temperature, can be admitted to the reactor at total pressures up to ~2 atmospheres. This treatment was found to be necessary to remove traces of impurity carbonyls. Generally, the reactor can be evacuated from a high pres-

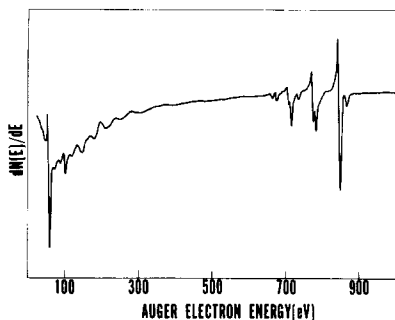


FIG. 2. AES of clean Ni(100) catalyst following oxidation at 1400 K in $P_{O_2} = 1.0 \times 10^{-6}$ Torr and reduction at 800 K in $P_{H_2} = 5$ Torr.

sure following a reaction and the catalyst surface assayed by AES within a 5-min period. The product CH_4 can be detected by opening a leak valve to the mass spectrometer in the surface analysis chamber or by extracting an aliquot into an evacuated gas chromatographic sampling loop. Gas chromatography (flame ionization detection) is the preferred technique because of its inherent sensitivity and because it avoids the ambiguity encountered in attempting mass spectrometric analysis in an ion-pumped vacuum system. Product detection capability using a small aliquot allows the measurement of a methane concentration corresponding to a monolayer on the Ni(100), 1-cm² sample. Hydrocarbon analysis was calibrated with standard gas mixtures and was found to be linear over the concentration range of interest and independent of the H_2/CO ratio.

Prior to each measurement of catalytic reaction rate, the Ni(100) surface was cleaned using an oxidation–reduction cycle (5). The crystal was first heated in O_2 at 1×10^{-6} Torr at ~ 1400 K to remove sulfur and carbon impurities. Subsequent reduction at 5 Torr H_2 and 800 K for 10 min resulted in an Auger spectrum free ($< 1\%$ of Ni 848 eV peak) of contaminants. Longer reduction times produced no significant change in surface area as measured by CO flash desorption. Significantly shorter reduction or no reduction at all gave rise to initially enhanced reaction rates which correlated

with an enhanced surface area as measured by flash desorption. Somorjai and Sexton have attributed an enhanced reaction rate of CO hydrogenation over Rh to the presence of subsurface oxygen (2). No evidence for reaction rate enhancement other than a surface area effect has been observed with the Ni(100) catalyst. The level of surface sulfur was maintained below the detectable limit (-0.1% of the 848 eV Ni peak) because of the sensitivity of the reaction rate to low levels of sulfur. The AES spectrum of a clean Ni(100) surface is shown in Fig. 2. This surface was the starting point for all kinetic measurements.

III. RESULTS AND DISCUSSION

Rate Measurements on Initially Clean Ni(100)

At a given temperature the rate of production of CH_4 over an initially clean cata-

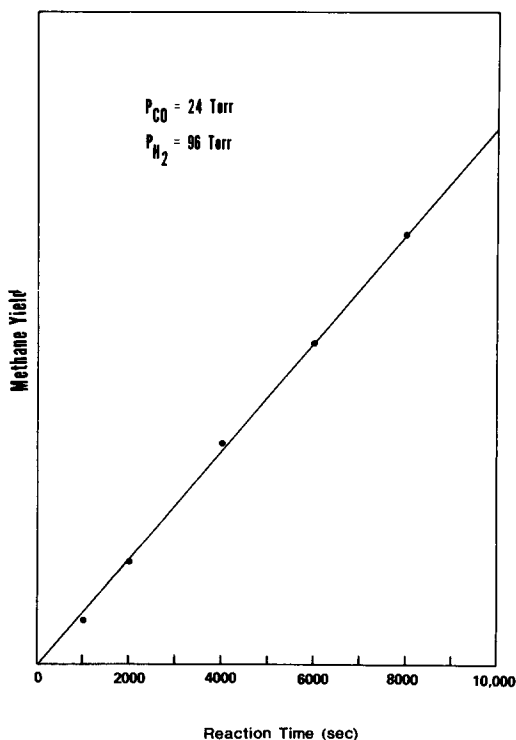


FIG. 3. Methane production over a Ni(100) catalyst as a function of reaction time. $H_2/CO = 4/1$, $P_T = 120$ Torr.

lyst crystal was extremely constant with no apparent induction period. This is demonstrated in Fig. 3 where the CH_4 yield is plotted as a function of reaction time. No self-poisoning was observed for reaction periods as long as 75 hr and conversions $< 5\%$. The specific rate or turnover number (CH_4/Ni surface atom/sec) was determined by an absolute measure of the amount of CH_4 produced ($< 1\%$) during a fixed time (typically 1000 sec), using the Ni(100) atom density (1.62×10^{15} atoms/cm 2) for the number of sites/cm 2 . These measurements were conducted over a period of many months using several crystal samples and the standard oxidation-reduction cleaning procedure. The reproducibility of specific rates measured in this manner was within 5%. The values of the specific methanation rate for a 4/1 H_2/CO ratio and total pressure of 120, 10, and 1 Torr are plotted in Arrhenius form in Fig. 4. The slope of the line obtained for the reaction at 120 Torr

corresponds to an activation energy of 24.7 kcal/mole. This value is in excellent agreement with the activation energies (25.5 and 26.1 kcal/mole) measured for supported nickel catalysts [e.g., see Vannice (8)]. In spanning the reaction temperature range 450–800 K, product methane yields traverse five orders of magnitude. It should be pointed out that reaction kinetics over such a wide temperature range are difficult if not impossible with high surface area materials due to heat and mass transfer limitations. Before discussing the pressure effects evident in Fig. 4 it is useful to introduce the AES characterization of an active crystal surface.

Formation of Surface "Carbide": Mechanistic Considerations

Auger spectroscopic analysis of the active Ni catalyst (Fig. 5a) following reaction at temperatures from 450 to 700 K and 120 Torr (4/1) H_2/CO pressure shows a "carbi-

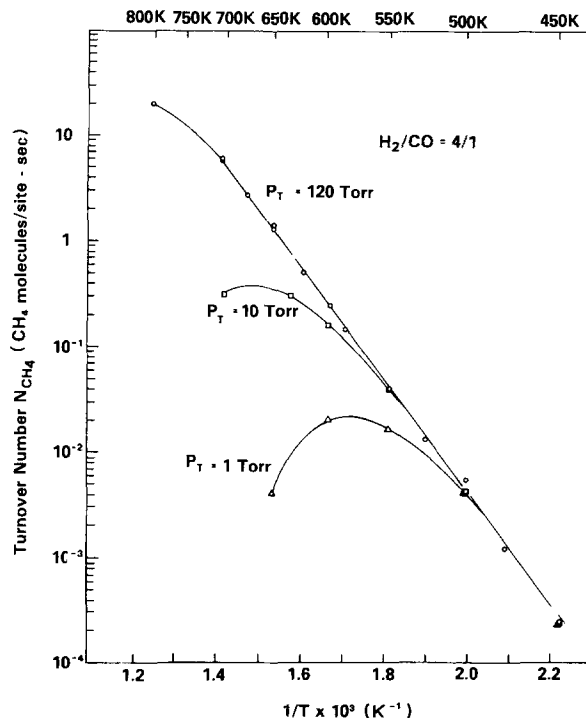


FIG. 4. Arrhenius plot of CH_4 synthesis (N_{CH_4}) on a Ni(100) at total reactant pressures of 1, 10, and 120 Torr. $\text{H}_2/\text{CO} = 4/1$.

dic" carbon on the surface consistent with 10–20% of a monolayer. The estimate of the coverage of "carbide" carbon is based on CO flash desorption results as well as Auger data obtained from a CO monolayer. The reaction kinetics of the catalyst containing this carbon were identical to those of initially clean Ni. Furthermore, this "carbide" carbon was easily removed by heating the crystal in H_2 ($P = 100$ Torr, 700 K). This surface carbon species can be produced in the absence of hydrogen by heating the crystal in pure CO. In separate experiments, a clean crystal was heated in 24 Torr CO for 1000 sec at 600 and at 700 K. Following heating at 600 K, the carbon AES spectrum shown in Fig. 5b was observed. As in the H_2/CO mixture (Fig. 5a),

no detectable oxygen was present following reaction. Continued heating in CO resulted in no further change in the carbon peak relative to the nickel peaks. Carbon formation by reaction with CO has been shown to occur on supported Ni and Ni films via the disproportionation reaction $2 CO \rightarrow C + CO_2$ (see Refs. 13 and 14). This carbide carbon could be removed by heating in H_2 (100 Torr). Following heating at 700 K, the carbon AES spectrum shown in Fig. 5c was observed. Continued heating in CO under these conditions resulted in a continuous increase in the carbon peak and a corresponding decrease in the nickel Auger peaks. This "graphitic" carbon species was not attenuated by heating in H_2 (100 Torr) at 650 K for a prolonged period.

The designations "carbide" and "graphitic" for these surface carbon species arise from the following considerations. The carbon AES peak shape from single crystal graphite (Fig. 6b), redrawn from Chang (7), is similar to that from the catalytically inactive nickel crystal produced by heating in CO at 700 K (Fig. 6a). Also, the carbon AES spectrum of nickel carbide (Fig. 6d), redrawn from Chang (7), is similar to that from the catalytically active crystal surface (Fig. 6c) found following reaction with H_2/CO at 450–800 K and with CO alone up to 650 K. The "carbide" species observed on an active crystal may be a hydrogenous species, since prior to Auger analysis the crystal was flashed *in vacuo* to ~650 K to remove any CO present. This procedure was required to avoid ambiguous results caused by electron beam damage of CO. This heat treatment may also lead to dissociation and desorption of other possible fragments, i.e., $CH_2 \rightarrow C(ads) + H_2$ (11, 12).

A kinetic study of the carbide carbon buildup in pure CO as well as its subsequent removal in H_2 (10) shows that the kinetic parameters associated with each of the above steps are comparable to those of the H_2/CO reaction mixture. These data suggest that not only is a surface carbide or

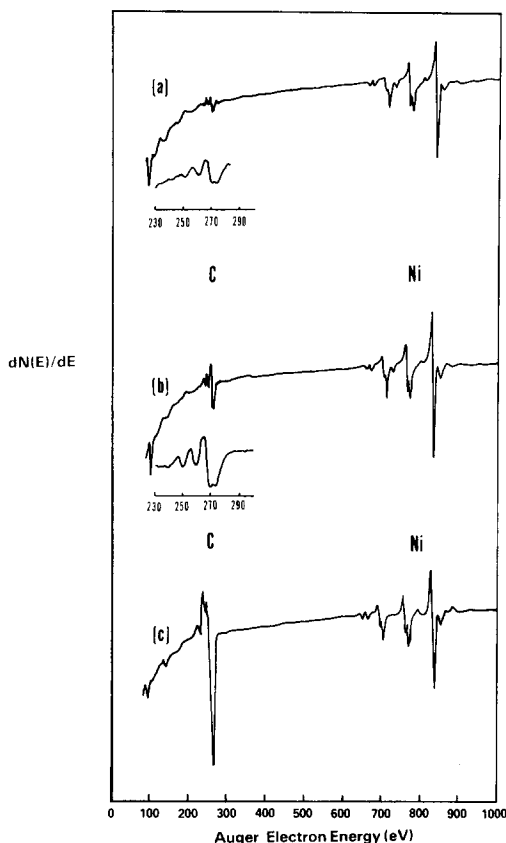


FIG. 5. AES spectra of Ni(100) crystal following: (a) Exposure to 120 Torr at 4 : 1 H_2 : CO mixture at 700 K after 10,000 sec. (b) Exposure to 24 Torr CO at 600 K. (c) Exposure to 24 Torr CO at 700 K.

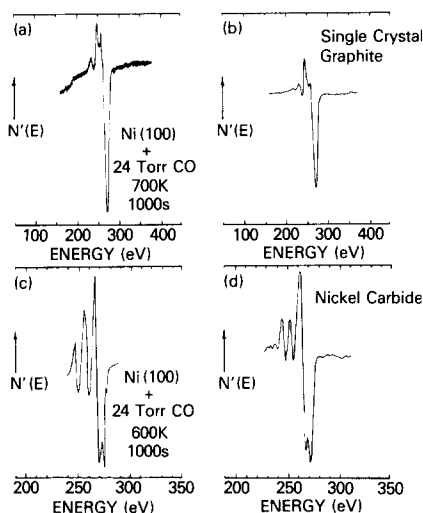


FIG. 6. Comparison of AES carbon signals on Ni(100) crystal with those from single crystal graphite and nickel carbide. (a) Following 1000 sec heating at 700 K in 24 Torr CO. (b) Single crystal graphite. (c) Following 1000 sec heating at 600 K in 24 Torr CO. (d) Nickel carbide.

hydrogenated carbide a possible route to product but is quite likely a major route to methane production. Preliminary X-ray photoelectron spectroscopic data on polycrystalline Ni foil suggest that the carbon species present following reaction is a hydrogenated carbon rather than a "carbide" carbon (11). These results agree with those of Demuth and Ibach (12) demonstrating the stability of CH_x fragments on Ni at $T > 300$ K. The present data support the work of Wentreck *et al.* (13) and Araki and Ponc (14) who have reported the production and reactivity of a carbon species on Ni following heating in CO.

Pressure Effect on Reaction Rate

Lowering the total pressure from 120 Torr has a dramatic effect on the rate of methanation (Fig. 4). At 120 Torr, linear Arrhenius behavior is observed up to ~ 700 K. At 10 Torr, a departure from Arrhenius linearity occurs at ~ 550 K at which temperature the rate of methane production begins to plateau. At 1 Torr, the rate begins to turn over at an even lower temperature (~ 485 K). This behavior is believed to arise be-

cause of the relationship between temperature, pressure, and the surface hydrogen atom (H_{ads}) concentration on the catalyst. At a given temperature, the concentration of H_{ads} increases with increasing hydrogen pressure until saturation is achieved. Maximum hydrogenation of CO occurs at this saturation point which falls on the linear Arrhenius line and further increase of pressure has little effect on the reaction rate. The rate data indicate near first order behavior of surface hydrogen coverage with total hydrogen pressure until saturation. Model calculations for hydrogen coverage (θ_{H}) as a function of temperature (T) and pressure (P) using data from Ertl *et al.* (15) predict a θ_{H} vs T, P behavior at reaction conditions analogous to the observed Ni(100) catalytic methanation rate vs T, P , supporting the above conclusion. A qualitatively similar behavior of rate versus hydrogen pressure has been observed for the hydrogenation of benzene on Ni/SiO₂ (16) as well as carbon deposition from a hydrogen/propylene mixture on nickel (17). Perhaps in these cases as well the turning over of the rate correlates with the departure of the H_{ads} concentration from a critical value associated with the particular reaction conditions.

Concurrent with the drop in H_{ads} concentration below saturation is an increase in the carbide level observed following reaction. At 650 K and 10 Torr reaction mixture, the carbide level measured following reaction is comparable to the level seen after exposure to pure CO at 600 K. Likewise, at 1 Torr the turning over of the rate has associated with it an increase in the carbide level following reaction. Exposure of the Ni(100) catalyst to 10 Torr or less total pressure of 4/1 H_2/CO at temperatures greater than 650 K results in deactivation. AES inspection of the surface following such a reaction shows a mixture of carbide and graphite carbon to be present. These results suggest that formation of a relatively inactive graphite requires both a critical temperature (~ 650 K) and a prerequisite

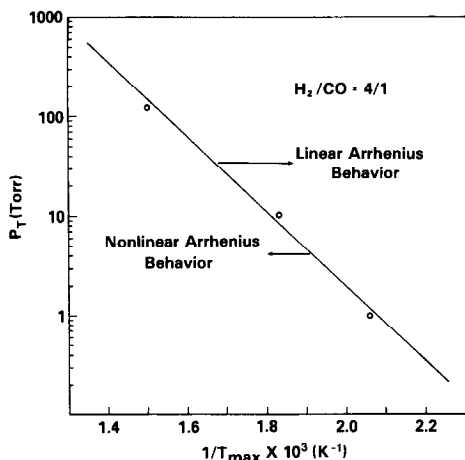


FIG. 7. A plot of the maximum temperature (T_{\max}) to which linear Arrhenius behavior is observed over a Ni(100) catalyst as a function of total reactant pressure (P_T). $H_2/CO = 4/1$.

surface carbide level. With a H_2/CO reaction mixture, hydrogen at a sufficient pressure to maintain an adequate surface concentration of H_{ads} , reduces the dynamic carbide level during reaction. At 120 Torr and 4/1 H_2/CO reaction mixture, the catalytic activity of the surface is maintained up to temperatures greater than 800 K with no evidence of graphite formation. However, if the hydrogen pressure is not sufficient to prevent accumulation of surface carbide, the critical carbide level can be exceeded. At reaction temperatures >650 K, this condition leads to rapid, multilayer graphite formation and catalytic inactivity.

Figure 7 shows the reciprocal of the maximum temperature to which linear Arrhenius behavior is observed as a function of total pressure for a 4/1 H_2/CO reaction mixture. Pressure-temperature combinations which fall above this line give rise to linear Arrhenius behavior. Conditions below this line can be expected to produce nonlinear Arrhenius data. This plot strongly suggests a hydrogen adsorption isostere on the Ni(100) surface under reaction conditions. The slope of this plot, corresponding to a desorption energy of 18.5 kcal/mole, compares with 23 kcal/mole H_2 desorption energy measured

by Ertl and co-workers for a clean Ni(100) surface (15). A reduction in H_2 desorption energy under reaction conditions is expected because of the presence of C(ads) and CO(ads) (14). This dependence of rate with total hydrogen pressure is likely to be a general phenomenon for other transition metal surfaces since hydrogen desorption energies change little from metal to metal. This suggests that at the onset of kinetic measurements pressure variation data should first be collected to ascertain if the total hydrogen pressure to be used is sufficient to give linear Arrhenius behavior throughout the temperature range of interest.

Reaction rates measured below 500 K exhibited near zero order behavior in total reactant pressure (4/1 $H_2 : CO$) in the pressure region from 1 to 1500 Torr. Data obtained at 503K and 625K are shown in Fig. 8. The results at 503K are consistent with the argument that a near saturation hydrogen coverage is present at 1 Torr reactant pressure, thus an increase in hydrogen pressure results in no substantial increase in $H(\text{ads})$. The results at 625K, in contrast, show a strong pressure dependence with an associated decrease in "carbide" carbon with increasing pressure. This observed near zero order behavior at 503K in total reactant pres-

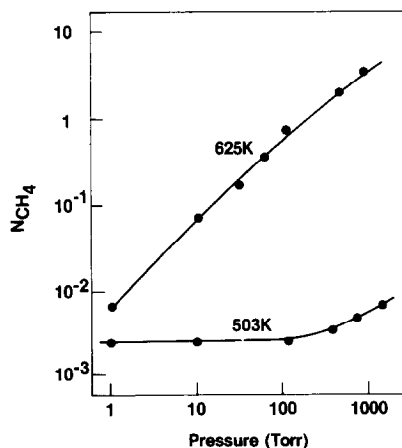


FIG. 8. Methane production as a function of total reactant pressure over a Ni(100) catalyst at a reaction temperatures of 503K and 625K ($H_2 : CO$ of 4 : 1).

sure over the single crystal catalyst contrasts with reported values near 0.5 for supported nickel catalysts by Vannice (8) and for Ni powders by Polizzotti *et al.* (4b). However, recent data for alumina-supported Ni reported by Vannice (18) over the total pressure range 1–10 atm display near zero order behavior in total pressure.

In Fig. 9 the methanation rate observed on a single crystal Ni(100) catalyst at 1 atmosphere reactant pressure is compared with the data acquired for Ni supported on alumina reported by Vannice (8). Generally speaking, a factor of 2 or 3 variation in the comparison of turnover numbers is assumed to be quite good, considering the errors involved in the measurement of reaction rates and actual surface areas. Thus there is excellent agreement between both the specific rates and activation energies measured for the single crystal Ni(100) catalyst and the high area supported catalyst.

At temperatures below 500 K, significant amounts of higher hydrocarbons were produced, both saturated and unsaturated. The amount and distribution over the single crystal Ni(100) catalyst agree with those observed by Vannice for dispersed Ni catalysts (8). At 1 atm, 503 K, and 4/1 H₂/CO, the Ni(100) catalyst yields 93% methane,

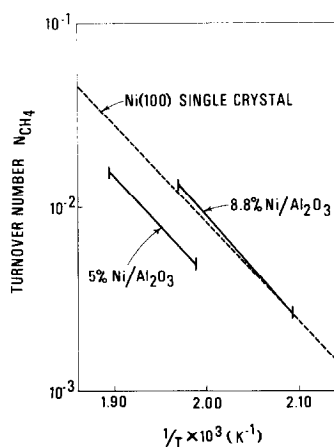


FIG. 9. A comparison of the rate of methane synthesis over a single crystal Ni(100) catalyst and supported Ni/Al₂O₃ catalysts at one atmosphere total reactant pressure.

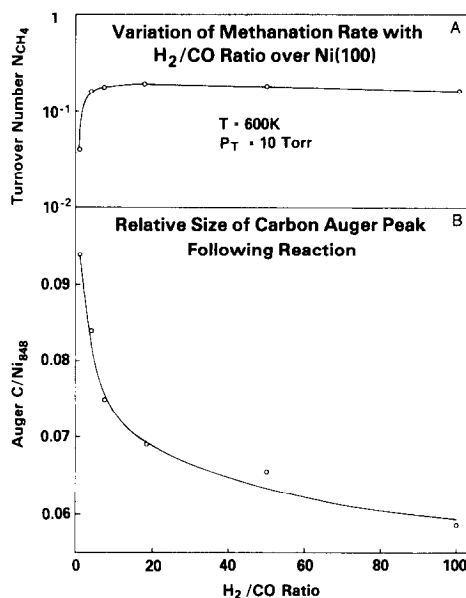


FIG. 10. (a) A plot of methane production as a function of H₂: CO ratio over a Ni(100) catalyst at 600 K and a total reactant pressure of 10 Torr. (b) A plot showing the size of the carbon AES peak relative to the Ni_{2p3/2} peak following reaction with various H₂/CO ratios.

6% C₂, 1% C₃, and 0.3% C₄⁺. The yields found by Vannice at 1 atm, 508 K, and 3/1 H₂/CO for 5% Ni/Al₂O₃ were 87% methane, 9% C₂, 3% C₃, and 1% C₄⁺.

Rate studies were also carried out varying H₂/CO ratios at a fixed total pressure of 10 Torr at 600 K. The observed turnover numbers as a function of mixture composition are shown in Fig. 10a. Methane production rises steadily from 1/1 to ~7/1 H₂/CO ratio and then changes very little out to ratios as high as 100/1. From the previous discussion of the rate variation with total hydrogen pressure, the surface hydrogen atom concentration is expected to be near saturation at this temperature–pressure condition. Small changes in total hydrogen pressure should produce little change in the rate of methane formed.

The corresponding carbide level following reaction with varying H₂/CO ratios is shown in Fig. 10b. At a H₂/CO ratio of 1/1 the carbide level measured is significantly higher than that seen following reaction

with a 4/1 H₂/CO mixture. As the partial pressure of hydrogen increases, the carbide level asymptotes to a nonzero value of C/Ni₈₄₈ = 0.06 (this is the peak height ratio of the 270 eV C peak to that of the Ni₈₄₈ peak). A C/Ni₈₄₈ ratio of 0.2 corresponds to ~0.5 monolayers of carbon as determined by AES inspection of a monolayer coverage of CO.

IV. SUMMARY

Detailed kinetic studies of the effect of total pressure, reactant partial pressure, and temperature on the turnover number for the hydrogenation of CO on a clean single crystal Ni(100) catalyst have demonstrated that:

(1) The turnover number measured on the single crystal (site density derived from the Ni atom density of a (100) plane) is in good agreement with values reported for high area supported catalysts (site density derived from chemisorption data).

(2) Under conditions of pressure and temperatures such that saturation hydrogen coverage is maintained on the surface: The variation of turnover number with temperature follows a strictly linear Arrhenius behavior in the range 450–700 K with an $E_a = 24.7$ kcal/mole.

(3) AES analysis of an active catalyst surface indicates a low level of a carbon species and the absence of oxygen. The AES lineshape of this carbon species has the distinctive characteristics of a carbidic species.

(4) A mechanism which involves the hydrogenation of an active carbon species is most consistent with these kinetic data. A detailed report of the hydrogenation kinetics will be published elsewhere.

ACKNOWLEDGMENTS

We acknowledge with pleasure the partial support of

this work by the Department of Energy, through the Division of Basic Energy Sciences.

REFERENCES

1. Kahn, P. R., Petersen, E. E., and Somorjai, G. A., *J. Catal.* **34**, 294 (1974).
2. Sexton, B. A., and Somorjai, G. A., *J. Catal.* **46**, 167 (1977); Krebs, H. J., and Bonzel, H. P., *Surface Sci.* **88**, 269 (1979).
3. Dwyer, D. J. and Somorjai, G. A., *J. Catal.* **52**, 291 (1978).
4. (a) Kelley, R. D., Revesz, K., Madey, T. E., and Yates, J. T., Jr., *Appl. Surface Sci.* **1**, 266 (1978). (b) Polizzotti, R. S., Schwarz, J. A., and Kugler, E. L., "Proc. of Symposium on Advances in Fischer-Tropsch Chemistry," Amer. Chemical Soc., Anaheim Meeting, 1978.
5. (a) Goodman, D. W., Kelley, R. D., Madey, T. E., and Yates, J. T., Jr., "Proc. of Symposium on Advances in Fischer-Tropsch Chemistry," Amer. Chemical Soc., Anaheim Meeting, 1978 (b) Madey, T. E., Goodman, D. W., and Kelley, R. D., *J. Vac. Sci. Tech.* **16**, 433 (1979).
6. (a) Joyner, R. W., *J. Catal.* **50**, 176 (1977). (b) Ponec, V., *Catal. Rev.-Sci. Eng.* **18**, 151 (1973).
7. Chang, C. C., "Analytical Auger Electron Spectroscopy, Characterization of Solid Surfaces" (P. F. Kane and G. B. Larrabee, Eds.). Plenum Press, New York, 1974.
8. Vannice, M. A., *J. Catal.* **44**, 152 (1976).
9. (a) Schouten, F. C., Ph.D. Thesis, Univ. of Utrecht, 1979. (b) Schouten, F. C., Te Brake, E., Gijzeman, O. L. J., and Bootsma, G. A., *Surface Sci.* **74**, 1 (1978).
10. Goodman, D. W., Kelley, R. D., Madey, T. E., and White, J. M., *J. Catal.*, submitted for publication.
11. Erickson, N., unpublished data.
12. Demuth, J. E., and Ibach, H., *Surface Sci.* **78**, L238 (1978).
13. Wentreck, P. R., Wood, B. J., and Wise, H., *J. Catal.* **43**, 366 (1976).
14. Araki, M., and Ponec, V., *J. Catal.* **44**, 439 (1976).
15. Christmann, K., Schober, O., Ertl, G., and Neumann, M., *J. Chem. Phys.* **60**, 4528 (1974).
16. van Meerten, R. Z. C., and Coenen, J. W. E., *J. Catal.* **37**, 37 (1975).
17. Rostrup-Nielsen, J., and Trimm, D. L., *J. Catal.* **48**, 155 (1977).
18. Vannice, M. A., and Garten, R. L., *J. Catal.* **56**, 236 (1979).